

# Comparison of diffusion coefficients for matched pairs of macrocyclic and linear molecules over a drug-like molecular weight range†

Andrew R. Bogdan,<sup>a</sup> Nichola L. Davies<sup>b</sup> and Keith James<sup>\*a</sup>

Received 20th June 2011, Accepted 5th September 2011

DOI: 10.1039/c1ob05996c

The diffusion coefficients of a series of closely matched pairs of macrocyclic and linear molecules have been compared using NMR spectroscopy. The macrocyclic series was designed both to overlap with and extend beyond the molecular weight range typically employed for drug-like molecules. The linear molecules each represent a carbogenic fission of their macrocyclic counterparts, designed to minimize differences in functionality and physicochemical properties. Each series of molecules was prepared using copper catalyzed azide-alkyne cycloaddition (CuAAC) reactions conducted in a flow using a copper tube. The macrocyclic series exhibited consistently higher diffusion across the entire molecular weight range studied. The fold difference in diffusion coefficients between the macrocyclic and linear analogues appeared to be independent of either solvent viscosity or dielectric environment.

## Introduction

Cyclization of a linear molecule into a macrocyclic ring constitutes a significant change in molecular shape. This transformation restricts the degrees of conformational freedom of the molecule,<sup>1</sup> and imposes structural organization which was absent in the linear precursor. The introduction of this conformational constraint comes at a synthetic cost, since macrocyclization reactions are typically conducted under high dilution conditions in order to avoid competing dimerization reactions.<sup>2,3</sup> The pre-organized shape of macrocycles has been used extensively in the fields of molecular recognition,<sup>4</sup> supramolecular chemistry,<sup>5</sup> and molecular self-assembly.<sup>6</sup> They are found widely in natural products,<sup>7</sup> and a number of natural product-derived macrocycles, such as cyclosporin,<sup>8</sup> are used as therapeutic agents, where they appear to defy conventional wisdom regarding the relationship between molecular size and drug-like behavior.<sup>9</sup> Consequently, there is growing interest in the design of macrocycle-based drugs,<sup>10</sup> particularly as a strategy for addressing those challenging molecular targets which involve an interaction between large protein interfaces,<sup>11</sup> where it might be necessary to deploy molecules well outside the conventional drug-like molecular weight range.

As part of a program exploring the use of macrocycle-based systems to address biological problems, we have begun to characterise the differences in physicochemical properties of macrocycles in comparison to their linear counterparts. We were especially interested in determining the impact of macrocyclization on

diffusion rate, which represents a sensitive measure of molecular shape,<sup>12</sup> and is an important determinant of behavior in different physicochemical or biological environments. Previous studies comparing the diffusion coefficients of macrocyclic *versus* linear molecules have compared either polymeric systems,<sup>13</sup> or macrocycles generated *via* chemical cyclization of a linear precursor.<sup>14</sup> In the former case, the molecules are comprised of simple, repeating units, *e.g.* alkanes and siloxanes, which lack the range of functional groups typically found in biologically active molecules. In the latter case, the creation of the macrocycle entailed significant changes in structure, such as the number of hydrogen-bonding groups present and the overall charge of the molecule. Since these will affect the interaction with the surrounding medium, they do not provide an unambiguous assessment of the direction and magnitude of the resultant change in diffusion coefficient for the system.

In order to explore the impact of macrocyclization on diffusion behavior in molecules more representative of biologically active agents, whilst avoiding the confounding effects of unintended structural changes, we have examined diffusion rates in a carefully matched set of macrocycles and linear analogues. We designed a series of macrocycles which would overlap with, and extend beyond, the molecular weight-range usually associated with drug molecules, which would possess functional groups commonly found in biologically active agents, and which provided an approximately linear relationship between molecular weight and ring size. We also designed a corresponding set of 'acyclic controls', generated by carbogenic fission of each macrocycle,<sup>15</sup> which provided an almost identical match with regard to functionality and molecular weight. Herein we report the results of studies comparing the diffusion behavior of these two types of molecule in three different solvent systems, representing a range of viscosities and dielectric environments, using the bipolar pulse longitudinal eddy current delay (BPPLD) NMR method.<sup>16</sup>

<sup>a</sup>Department of Chemistry, The Scripps Research Institute, 10550 N. Torrey Pines Road, La Jolla, California, USA. E-mail: kjames@scripps.edu; Fax: +1 858 784 7550; Tel: +1 858 784 2507

<sup>b</sup>Pfizer Worldwide Research, Sandwich, Kent, CT13 9NJ, UK

† Electronic supplementary information (ESI) available: Full synthetic procedures, compound characterization, <sup>1</sup>H and <sup>13</sup>C NMR spectra and NMR diffusion data. See DOI: 10.1039/c1ob05996c

## Results and discussion

### Macrocycle and acyclic control design

We designed a series of macrocycles and acyclic controls which covered 12- to 29-membered rings and molecular weights from 300 to 730 respectively, and which could be synthesized efficiently using copper catalyzed azide-alkyne cycloaddition (CuAAC) reactions under flow, which we have reported recently (Fig. 1).<sup>17</sup> This range of ring sizes encompassed the most common size found in a recent survey of natural products (14-membered),<sup>7</sup> and approached the size of cyclosporin itself (33-membered).<sup>8</sup> The molecular weight range extended well beyond that reflected in well-established guidelines for orally bioavailable drugs ( $500 \text{ g mol}^{-1}$ ).<sup>9</sup> As illustrated in Fig. 2a, in order to maximize the chance of detecting a small effect on diffusion behavior, we also built into

our design an approximately linear relationship between molecular weight and ring size.

We also designed the systems to feature drug-like functional groups (amides, ethers, aryl/heteroaryl rings and stereocenters) and physicochemical properties. Fig. 2b illustrates one important measure of the drug-like properties of these systems, lipophilicity, which reflects the affinity of a molecule for a lipid environment. The lipophilicity of the macrocyclic set, as reflected in their  $\log D_{7.4}$  values,<sup>18</sup> lies within a typical range for drug-like molecules.<sup>19</sup>

The acyclic controls were designed to represent a carbogenic fission of their macrocyclic counterpart,<sup>15</sup> which fully preserved the functionality of the macrocycle and yielded an almost identical MW. Thus, alkyl fragments were incorporated within the macrocycle framework to allow at least one carbon-carbon bond-scission

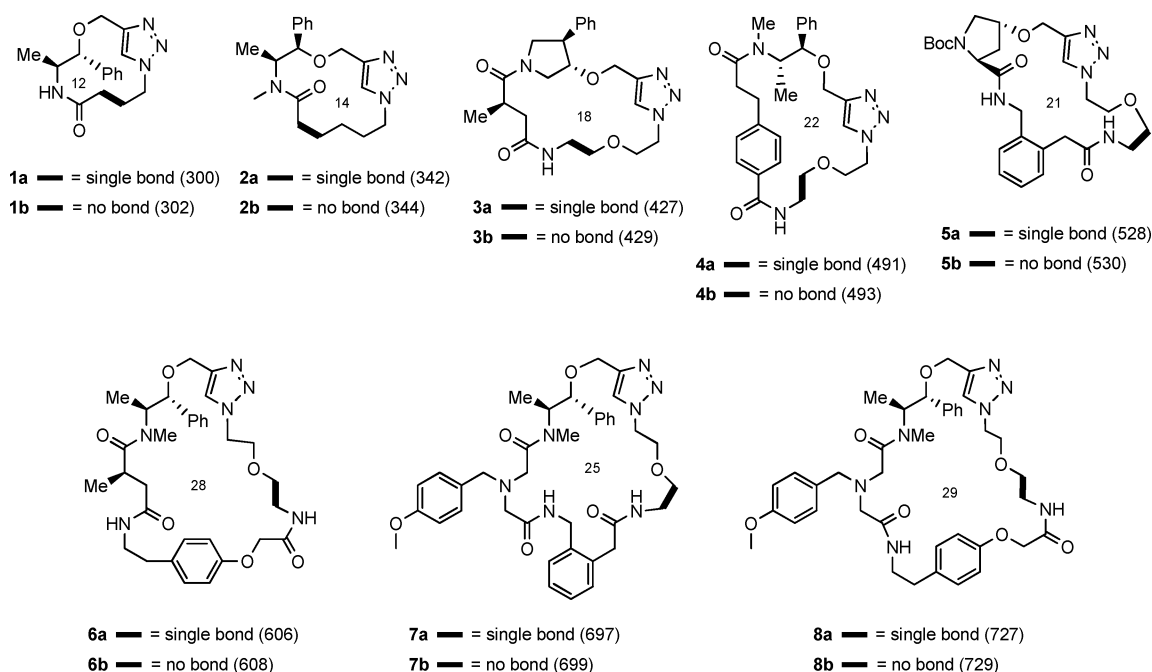


Fig. 1 Matched pairs of macrocycles and acyclic controls. Ring size indicated within macrocyclic ring. Molecular weight indicated in parenthesis.

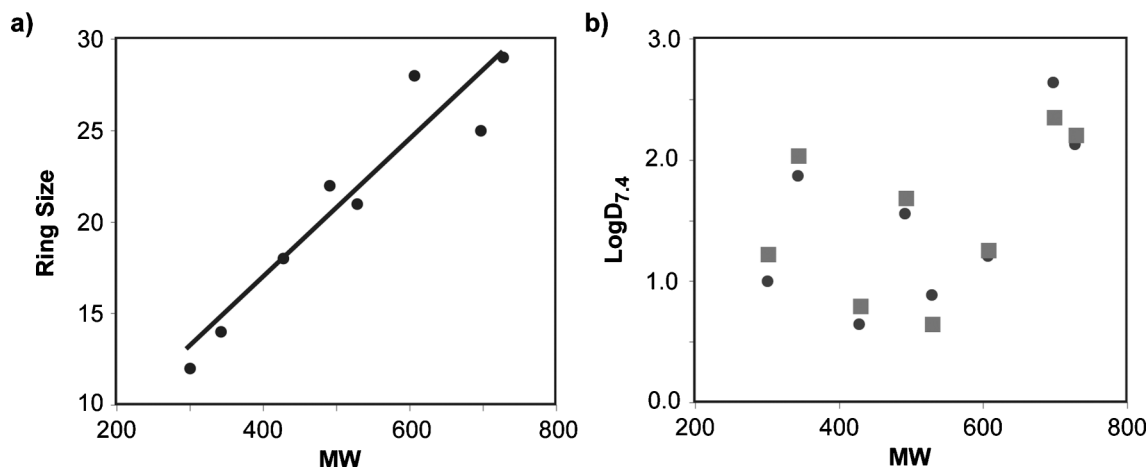
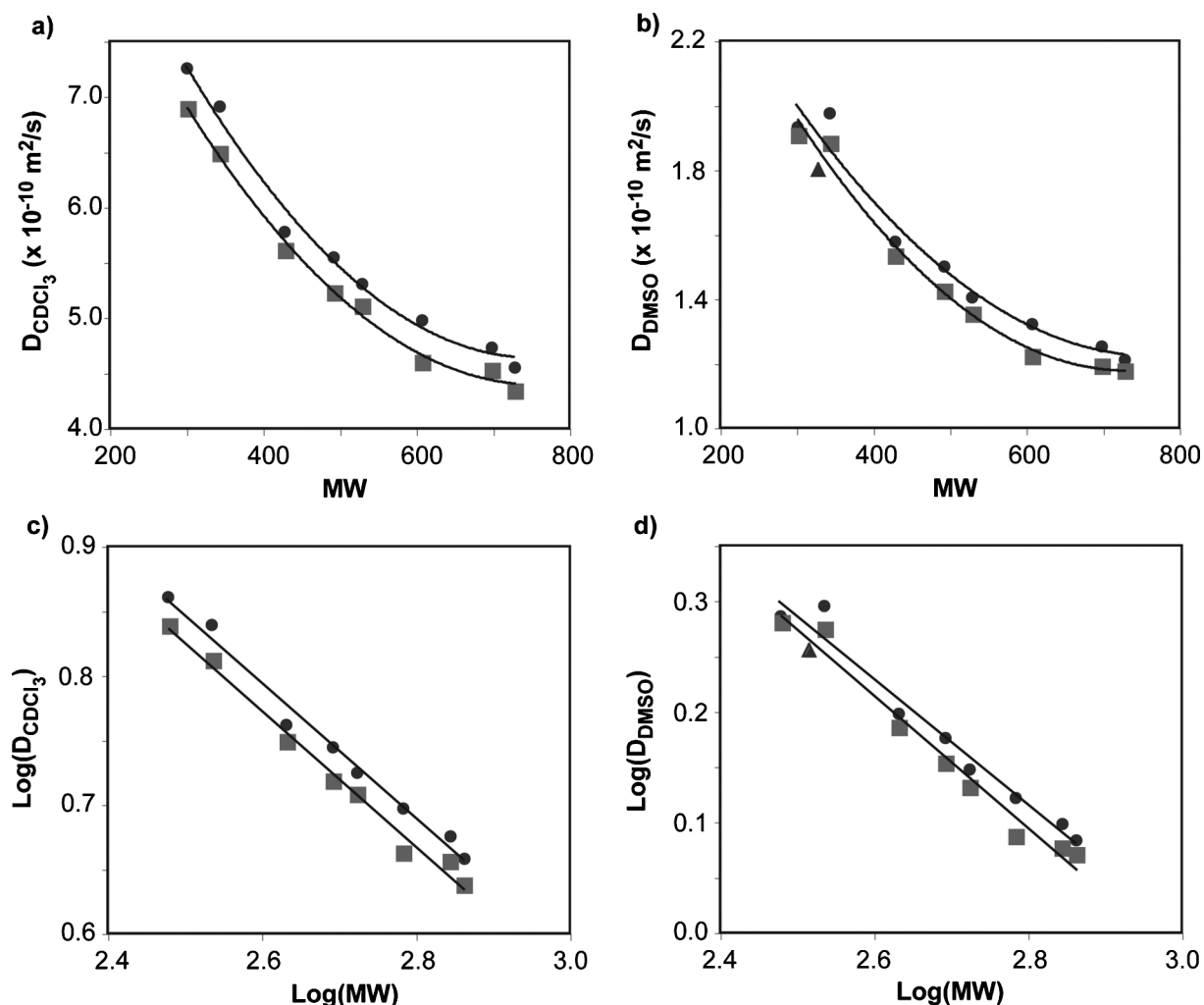


Fig. 2 (a) A plot of ring size versus MW for macrocycle series,  $R^2 = 0.90$  for linear fit. (b) A plot of  $\log D_{7.4}$  versus MW for matched pairs of macrocycles (circles) and acyclic controls (squares). Each matched pair shares approximately the same MW.



**Fig. 3** Diffusion data comparing macrocycles (circles) and acyclic controls (squares). The triangle denotes data point for the des-methyl analog of **2a**. Error bars are obscured by the data points. (a) A plot of the diffusion coefficient in CDCl<sub>3</sub> ( $D_{CDCl_3}$ ) versus MW. (b) A plot of the diffusion coefficient in *d*<sub>6</sub>-DMSO ( $D_{DMSO}$ ) versus MW. (c) A plot of  $\text{log}(D_{CDCl_3})$  versus  $\text{log}(MW)$ . (d) A plot of  $\text{log}(D_{DMSO})$  versus  $\text{log}(MW)$ ;  $R^2$  for logarithmic plots combining all data across both solvents = 0.99,  $p < 0.001$ .

which did not generate a significant functional group change. The success of this approach is evident in the close correspondence of  $\text{log}D_{7.4}$  values for the macrocyclic and acyclic control pairs, indicating that there has been no significant change in lipophilicity upon macrocyclization (Fig. 2b).

### Macrocycle and acyclic control synthesis

The macrocycles were synthesized *via* a copper catalyzed azide-alkyne cycloaddition (CuAAC), or ‘click’ reaction, conducted in flow,<sup>17</sup> typically affording >100 mg quantities of product under modest dilution (0.017 M) conditions. The azido-alkyne precursor for each macrocycle was synthesized in a short, modular synthetic sequence from commercially available, homochiral fragments. The acyclic controls were also synthesized in flow *via in situ* generation of each alkyl-azide reactant,<sup>20</sup> utilizing common intermediates from the corresponding macrocycle synthesis wherever possible (see Supporting Information for synthetic sequences and full experimental details†).

### Diffusion studies

Diffusion coefficients for the entire set of molecules were measured in 10 mM CDCl<sub>3</sub> and *d*<sub>6</sub>-DMSO solutions, using the bipolar pulse longitudinal eddy current delay (BPPLD) method (see Supporting Information for full experimental details†).<sup>16</sup> These solvents were chosen as models for the low (CDCl<sub>3</sub>, 4.8) and high (*d*<sub>6</sub>-DMSO, 46.7) dielectric environments encountered in physiological systems, whilst enabling complete dissolution of all the compounds examined at the necessary concentrations, which was not possible in pure D<sub>2</sub>O. These solvents also afforded two different viscosities for the diffusion medium, in order to confirm that any effects on the diffusion rate were independent of this parameter.

The observed diffusion coefficients were highly reproducible (see Supporting Information for full set of diffusion data†). Fig. 3 depicts the observed diffusion coefficients plotted *versus* molecular weight, for CDCl<sub>3</sub> and *d*<sub>6</sub>-DMSO. The results demonstrate an expected inverse relationship between MW and diffusion coefficient in both solvent systems. Most importantly, they also

illustrate a clear increase in diffusion rate for the macrocyclic series *versus* the acyclic controls, which is highly statistically significant (5% increase for macrocycle series,  $R^2 > 0.99$ ,  $p < 0.001$  for the combined data across both solvents; see experimental section for details of statistical treatment). In fact, every macrocycle examined exhibits a higher diffusion rate than its acyclic counterpart. The diffusion rates are some 3.5-fold higher in  $\text{CDCl}_3$ , compared to  $d_6$ -DMSO, reflecting the higher viscosity term  $\eta$  for  $d_6$ -DMSO (2.0 cP) *versus*  $\text{CDCl}_3$  (0.54 cP) in the Stokes–Einstein equation:<sup>12,21</sup>

$$D = \frac{kT}{6\pi\eta r_{\text{H}}}$$

The data also demonstrate that, for these examples, the effect is present at both low MW (300) and high MW (730), well beyond the Lipinski Rule-of-Five range.<sup>9</sup> The effect is modest in absolute terms, averaging a change of +5% in  $\text{CDCl}_3$ , and translates to a macrocycle of MW 550 exhibiting the diffusion behavior of a linear molecule of MW 500.

Our findings differ from those of earlier studies in terms of the magnitude of observed increase in diffusion rates upon macrocyclization. Thus, a comparison of the diffusion rates for macrocyclic *versus* linear siloxane polymers in toluene found a ratio of  $0.85 \pm 0.01$  for the diffusion coefficients  $D_{\text{l}}/D_{\text{r}}$  of the linear (l) and ring (r) molecules respectively.<sup>13b</sup> This is within experimental error of the theoretical ratio of  $8/3\pi$  (0.85) predicted for cyclic *versus* linear molecules in the absence of free-draining and excluded volume effects.<sup>13d</sup> In comparison, the average ratio  $D_{\text{l}}/D_{\text{r}}$  in  $\text{CDCl}_3$  for the macrocycles and acyclic controls in our study is  $0.95 \pm 0.01$ , suggesting that excluded volume effects are more significant in these more drug-like molecules compared to simple polymers. Interestingly, the ratio of sedimentation coefficients  $s_{\text{l}}/s_{\text{r}}$  for linear and nicked DNA for polyoma virus,<sup>22</sup> and  $\lambda$ DNA,<sup>23</sup> was found to be 0.91 and 0.88 respectively. Since sedimentation coefficient  $s$  is directly proportional to diffusion coefficient  $D$ ,<sup>13b</sup> this ratio is directly comparable to  $D_{\text{l}}/D_{\text{r}}$ . These ratios for cyclic *versus* linear DNA molecules therefore fall between the value that we have observed and the value reported for cyclic *versus* linear polydimethylsiloxane.

The closeness of the ratio  $D_{\text{l}}/D_{\text{r}}$  to unity for our experiments suggests that the acyclic molecules probably do not exist in a fully extended, ‘rod-like’, conformation, and instead undergo some form of hydrophobic collapse to a more compact structure.<sup>24</sup> Furthermore, the macrocyclic systems, despite the conformational constraint imposed by the ring, probably still retain a considerable degree of flexibility. Nevertheless, the consistency of the effect is striking and whilst the differences in diffusion coefficients between macrocycles and acyclic controls are small, they are statistically significant.

As illustrated in Fig. 3a and 3b, a logarithmic plot of the data from both series of molecules and in both solvents is a straight line, which fits the equation:

$$D = C(\text{MW}) - 0.56 (\pm 0.079)$$

(where  $D$  = diffusion coefficient and  $C$  is a constant) extremely well ( $R^2 = 0.99$ ,  $p < 0.001$ ). This quantitative relationship between the logarithm of diffusion coefficient and the logarithm of MW is consistent with previous studies examining small molecule

diffusion in  $\text{CDCl}_3$ .<sup>25</sup> The consistency of slope, regardless of solvent or molecular series, is noteworthy.

### Solvent effects

It appears in Fig. 3b and 3d that the components of matched pair **2** (MW 340 and 342), although fitting the general trend of higher diffusion rate for the macrocycle, are outliers from the line in  $d_6$ -DMSO. This is the only pair which does not possess an amide N–H group, the *N*-methyl analog having been chosen to provide a larger MW increment over pair **1**. Since pair **2** is not an outlier in  $\text{CDCl}_3$  (Fig. 3a), we hypothesized that in  $d_6$ -DMSO, the absence of an amide N–H group meant less interaction with solvent and therefore a resultant boost in diffusion rate compared to closely related molecules which do possess an amide N–H group. The corresponding des-methyl analog,<sup>26</sup> of macrocycle **2a** was therefore examined in both  $\text{CDCl}_3$  and  $d_6$ -DMSO. Pleasingly, the measured diffusion coefficient for this molecule in  $d_6$ -DMSO was lower (Fig. 3b and d) and more in line with the other members of the macrocyclic series, thereby yielding an improved fit for the curve ( $R^2 = 0.99$  *versus* 0.97, when the des-methyl analog was substituted for **2a**; data included in Supporting Information†). This result is consistent with reports of lower diffusion rates in  $d_6$ -DMSO *versus*  $\text{CDCl}_3$  for molecules which can form hydrogen-bonds to DMSO.<sup>27</sup> It also highlights the challenges of designing a compound test set which provides smooth structural variation over a wide MW range, as well as access to relevant controls and which can be synthesized efficiently. It also indicates that macrocycles of much different structure or polarity compared to those studied here might exhibit a different y-intercept for the graphs of diffusion coefficient *versus* MW.

In order to confirm that these shape-driven changes in diffusion coefficient would also be observed under more physiological conditions, we measured the diffusion coefficients of selected pairs in an aqueous medium, adding the minimum possible quantity of DMSO in order to maintain solubility. Thus, Fig. 4 shows the diffusion coefficients for pairs **1**, **3**, **5** and **8** in a 2.5 mM  $\text{D}_2\text{O} : d_6$ -DMSO (9 : 1) solution. The macrocyclic examples show the same statistically significant increase in diffusion rate compared to their matched acyclic controls as we had observed in the other solvent systems.

Comparing the diffusion coefficients for this set of four macrocycles (**1a**, **3a**, **5a** and **8a**) across the three different solvent systems examined, it is apparent that the diffusion coefficients under aqueous conditions fall between those measured in  $\text{CDCl}_3$  and  $d_6$ -DMSO, as would be expected based upon their viscosities (Fig. 5). Thus, we feel confident that the differences in diffusion rates we have observed for the macrocyclic *versus* acyclic control series would be observed in any media which possess a viscosity in this range.

Comparing the slopes of the lines in Fig. 5, whilst the slopes in  $\text{CDCl}_3$  and  $d_6$ -DMSO are the same, the slope of the line in  $\text{D}_2\text{O} : d_6$ -DMSO (9 : 1) is more shallow (statistically significant difference), indicating that in this medium there is less reduction in diffusion coefficient as molecular weight increases. This could be a consequence of the higher dielectric nature of this aqueous system, resulting in more hydrophobic collapse of the lipophilic substituents in the larger, more flexible molecules,<sup>24</sup> and therefore

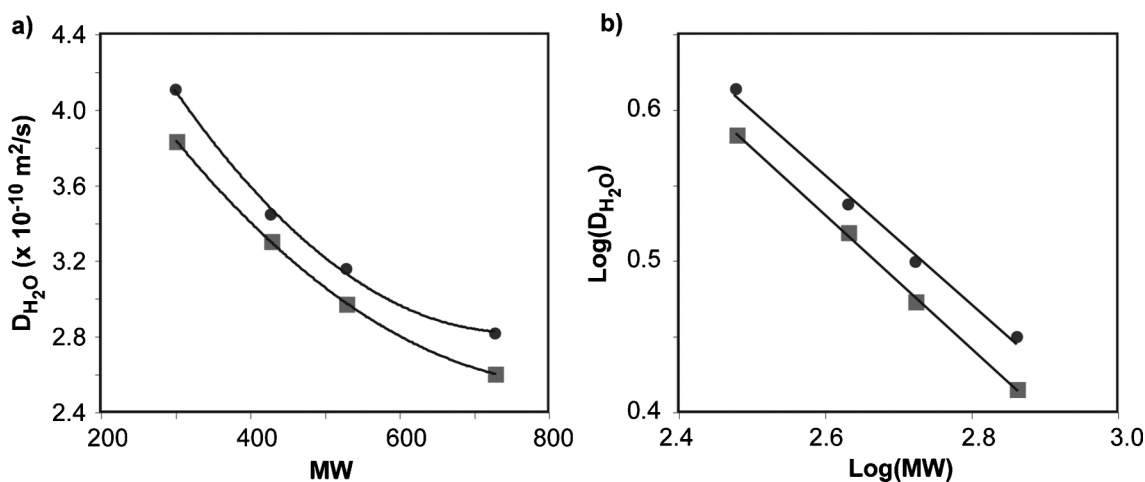


**Fig. 4** Diffusion data comparing macrocycles (circles) and acyclic controls (squares). a) A plot of the diffusion coefficient in  $D_2O:d_6\text{-DMSO}$  (9:1) ( $D_{H_2O}$ ) versus MW. b) A plot of  $\text{log}(D_{H_2O})$  versus  $\text{log}(MW)$ ;  $R^2$  for logarithmic plots = 0.99,  $p < 0.001$ .

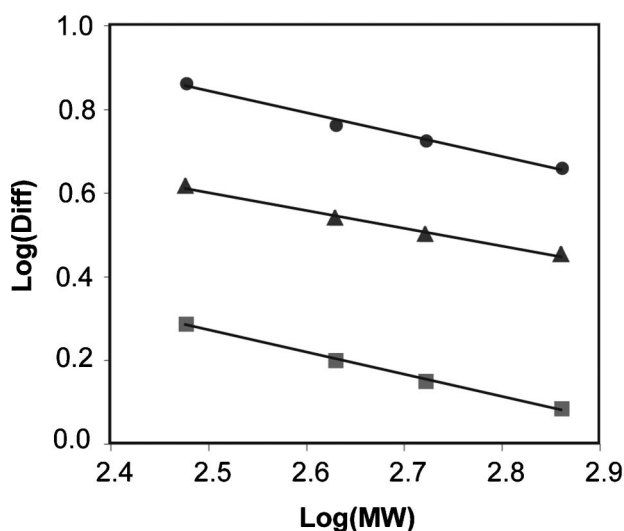


**Fig. 5** A plot of the logarithms of the diffusion coefficients in  $CDCl_3$  (circles),  $D_2O:d_6\text{-DMSO}$  (9:1; triangles) and  $d_6\text{-DMSO}$  (squares) for macrocycles **1a**, **3a**, **5a** and **7a** versus the logarithm of MW.

(in comparison to the other solvents) more compact structures with lower hydrodynamic radius and higher diffusion coefficient.

## Conclusions

We have shown that macrocyclization of polyfunctional, non-polymeric molecules in the molecular weight range 300–730, generating systems with 12- to 29-membered rings, results in a statistically significant increase in diffusion coefficient. This effect is evident across this entire range of molecular weight and ring size examined. It also appears to be independent of solvent viscosity and solvent dielectric over the range studied. The magnitude of increase in diffusion coefficient for the macrocyclic series is smaller than observed in simpler, more uniform oligomers such as alkanes, poly(dimethoxysiloxanes) or even DNA. This suggests that for this set of matched pairs, the molecular volumes occupied by the ensemble of conformations for the linear systems and the

macrocycles are very similar. There appears to be no support for a model in which the acyclic systems exhibit an extended, rod-like structure and the macrocycles possess a compact, spheroidal structure.

Although the systems examined here point the way towards a general strategy for increasing the diffusion rate of drug-like structures *via* macrocyclization, they are still relatively simple models of the therapeutically important macrocyclic natural products such as cyclosporin. Thus, whilst they are macrocyclic and possess a similar lipophilicity, they are still lower in molecular weight, and perhaps most importantly, they possess neither the superb network of trans-annular intramolecular hydrogen bonds observed in this natural product, nor its array of *N*-methylated amide bonds.<sup>8</sup> We suspect therefore that a macrocyclic structure, whilst important to the success of such agents, constitutes just one component in a set of structural features which operate in concert to confer drug-like behavior.

Future studies will therefore examine still higher MW systems, as well as the impact of introducing intramolecular hydrogen-bonds, in an effort both to constrain these systems further and ‘conceal’ polar functional groups within the molecule. We will also expand our studies beyond the measurement of diffusion rates to include the impact of macrocyclization on passage through both synthetic and biological membranes.

## Experimental procedures

### General considerations

All reagents and solvents were used as received. THF was distilled from sodium. NMR spectra were recorded on Bruker DRX-600, Bruker DRX-500, or Bruker AMX-400 instruments using residual solvent peak as a reference. Data are reported as s = singlet, d = doublet, t = triplet, q = quartet, m = multiplet, br = broad. LC/MS analyses were carried out using an Agilent Technologies HPLC (Agilent Technologies 1100 Series diode array detector, Agilent Technologies 1100 Series column heater, Agilent 1100 Series pump, and Agilent 1100 Series degasser) interfaced with an Agilent Technologies 6110 Quadrupole LC/MS. Column chromatography was performed using a Biotage Horizon automated



flash chromatography system equipped with a Biotage Horizon detector, fraction collector and pump where noted.

### NMR diffusion coefficient determination

All the NMR experiments were acquired on a Bruker Avance 600 MHz spectrometer, equipped with a 5 mm TCI cryoprobe with z-gradients capable of generating 54 G/cm field strengths. The temperature controller was set to 298 K with an air flow of 535 l h<sup>-1</sup> in order to avoid any temperature fluctuations due to sample heating during acquisition and to avoid sample vibrations from a high air-flow. Samples were made up to 10 mM solutions in DMSO-*d*<sub>6</sub> or CDCl<sub>3</sub> with some TMS vapour, and 180 μL of this solution was added to a 3 mm NMR tube to avoid problems of convection. In the case of samples in 10% DMSO in D<sub>2</sub>O, samples were made up at 2.5 mM and 600 μL of this solution was added to a 5 mm NMR tube. The lower concentration was required due to the limited solubility in this solvent. To maintain good signal to noise, the use of 5 mm NMR tubes is possible for more viscous solvents, as the onset of Rayleigh–Benard convection is ablated at the temperatures used during this investigation.

Diffusion coefficients were determined with a high degree of reproducibility on the NMR system used. Using robust statistical analysis, we have determined that the relative differences in diffusion between the linear and macrocyclic analogues are significant. However, the absolute accuracy of the diffusion coefficient as measured by NMR is limited by the accuracy of the calibration of the gradient and temperature, and often prone to errors introduced during the calculation method. Steps were taken to minimise these errors as detailed, however, it would be difficult to accurately compare diffusion coefficients between different NMR systems. The gradient strength was calibrated using the diffusion coefficient of water in a standard solution of 0.1 mg ml<sup>-1</sup> GdCl<sub>3</sub>, 0.1% DSS, 1% H<sub>2</sub>O in D<sub>2</sub>O. The values of the measured diffusion coefficient (*D*) of water, the known diffusion coefficient of water and the current gradient calibration value (*gc*(old)) were used to obtain the new gradient calibration value (*gc*(new)) using the following equation:<sup>28</sup>

$$gc(\text{new}) = gc(\text{old}) \times \sqrt{D(\text{measured})/D(\text{known})}$$

The temperature was calibrated with a sample of methanol-*d*<sub>4</sub> (99.8 at%), sealed under atmospheric pressure, using details described elsewhere.<sup>29</sup>

All DOSY experiments used the ledbpgp2s sequence (available in standard Bruker pulse sequence library). A gradient duration ( $\delta$ ) of 2 ms and an eddy current delay of 5 ms was used in all cases. The diffusion time (*t*) was 100 ms in the case of CDCl<sub>3</sub>, and 200 ms in the case of *d*<sub>6</sub>-DMSO and 10% *d*<sub>6</sub>-DMSO in D<sub>2</sub>O. In each PFG NMR experiment, a series of 16–32 spectra on 16 K data points were collected, using a linear gradient ramp from 5–95% of the maximum gradient strength.

After acquisition, the data was zero filled to 32k, Fourier transformed and baseline corrected in f2. The diffusion coefficients were calculated with the *T*<sub>1</sub>/*T*<sub>2</sub> relaxation module using mono-exponential fitting, rather than the 2D processing protocol. This is available in Bruker Topspin v.2. For each sample, several well resolved signals were used to extract individual diffusion coefficients (an example of the raw data and the fitting report is included in the Supporting Information†). These signals have

been averaged for each run in order to derive the diffusion coefficient and a standard deviation. Statistical analysis confirms that the variation in diffusion coefficient within each run is the same as the comparison between runs. Confidence intervals were determined based upon the observation that measurements on all the compounds were of equal precision, therefore a single estimate of variance was derived based upon the between-run differences for all compounds. The analysis demonstrates that a difference in diffusion coefficients between macrocycles and linear controls of 1% would be statistically significant. The observed difference of 5% is highly statistically significant.

TMS was included in the CDCl<sub>3</sub> and DMSO datasets as a control to check temperature was consistent in all experiments. As can be seen in the table of diffusion data, this is very reproducible and allows confidence in the comparison of data between macrocycles and linear analogues.

### General procedure for preparative scale flow macrocyclization

Azido-alkyne (0.10 M in EtOH, 100 μL, 0.010 mmol, 1.0 eq), TTTA (0.01 M in EtOH, 100 μL, 0.001 mmol, 0.10 eq), DIPEA (0.1 M in EtOH, 200 μL, 0.020 mmol, 2.0 eq) and EtOH (200 μL) were aspirated from their respective source vials, mixed through a PFA mixing tube (0.2 mm inner diameter), and loaded into an injection loop. The reaction segment was injected into the flow reactor set at 150 °C, passed through the reactor at 300 μL min<sup>-1</sup> (5 min residence time). A total of 40 reaction segments prepared in this manner were collected in a round bottom flask. Upon completion, the reaction mixture was concentrated and dried *in vacuo*. The crude reaction mixture was purified using a Biotage Horizon automated flash column chromatography system (silica gel, EtOAc, *R*<sub>f</sub> 0.17) to yield **1a** as a white solid (103.8 mg, 87% yield): <sup>1</sup>H NMR (600 MHz, CD<sub>3</sub>OD):  $\delta$  8.06 (br. s., 1 H), 7.64 (br. s., 1 H), 7.26–7.39 (m, 4 H), 7.19–7.25 (m, 1 H), 4.88 (d, *J* = 13.2 Hz, 1 H), 4.73 (br. s., 1 H), 4.39 (br. s., 1 H), 4.21 (d, *J* = 13.2 Hz, 2 H), 3.53 (d, *J* = 6.6 Hz, 1 H), 2.20–2.58 (m, 3 H), 1.97 (br. s., 1 H), 0.79 (d, *J* = 6.6 Hz, 3 H); <sup>13</sup>C NMR (150 MHz, CD<sub>3</sub>OD):  $\delta$  173.3, 147.3, 141.0, 129.5, 128.4, 128.3, 127.4, 77.5, 63.3, 52.8, 52.2, 34.2, 26.1, 11.6; HRMS (ESI-TOF): C<sub>16</sub>H<sub>20</sub>N<sub>4</sub>O<sub>2</sub>: [M + H]<sup>+</sup>: calculated 301.1659, found 301.1664.

### General procedure for preparative scale flow intermolecular CuAAC reaction

Alkyne (0.25 M in DMF, 150 μL, 0.038 mmol, 1.0 eq), iodoethane (0.50 M in DMF, 150 μL, 0.075 mmol, 2.0 eq), NaN<sub>3</sub> (0.30 M in DMF, 187.5 μL, 0.056 mmol, 1.5 eq) and DIPEA (0.5 M in DMF, 75 μL, 0.038 mmol, 1.0 eq) were aspirated from their respective source vials, mixed through a PFA mixing tube (0.2 mm inner diameter), and loaded into an injection loop. The reaction segment was injected into the flow reactor set at 150 °C, passed through the reactor at 150 μL min<sup>-1</sup> (10 min residence time). A total of 10 reaction segments prepared in this manner were collected in a round bottom flask. Upon completion, the reaction mixture was concentrated and dried *in vacuo*. The crude reaction mixture was purified using a Biotage Horizon automated flash column chromatography system (silica gel, 5% MeOH in CH<sub>2</sub>Cl<sub>2</sub>, *R*<sub>f</sub> 0.17) followed by PTLC (silica gel, 500 μm plates, 5% MeOH in CH<sub>2</sub>Cl<sub>2</sub>) to yield **1b** as an off-white solid (78.5 mg, 69% yield): <sup>1</sup>H NMR

(600 MHz, CDCl<sub>3</sub>):  $\delta$  7.44 (s, 1 H), 7.16–7.35 (m, 5 H), 6.56 (d,  $J = 7.2$  Hz, 1 H), 4.73 (d,  $J = 13.8$  Hz, 1 H), 4.39 (d,  $J = 2.4$  Hz, 1 H), 4.33–4.43 (m, 3 H), 4.15 (m, 1 H), 1.91 (s, 3 H), 1.52 (t,  $J = 7.2$  Hz, 3 H), 0.91 (d,  $J = 6.6$  Hz, 3 H); <sup>13</sup>C NMR (150 MHz, CDCl<sub>3</sub>):  $\delta$  169.7, 144.9, 138.7, 128.6, 127.8, 126.7, 121.9, 82.8, 62.7, 50.2, 45.5, 23.5, 15.6, 13.5; HRMS (ESI-TOF): C<sub>16</sub>H<sub>22</sub>N<sub>4</sub>O<sub>2</sub>: [M + H]<sup>+</sup>: calculated 303.1815, found 303.1823.

## Acknowledgements

This work was supported by a grant from Pfizer Pharmatherapeutics Research. The authors would like to thank Phil Brain (Pfizer) for statistics support and Lee Roberts (Pfizer) for advice and valuable discussions.

## Notes and references

- N. Go and H. Scheraga, H. A., *Macromolecules*, 1970, **3**, 178.
- L. A. Wessjohann and E. Ruijter, *Top. Curr. Chem.*, 2005, **243**, 137.
- G. Illuminati and L. Mandolini, *Acc. Chem. Res.*, 1981, **14**, 95.
- For selected examples see: (a) M. Krishnamurthy, K. Simon, A. M. Orendt and P. A. Beal, *Angew. Chem., Int. Ed.*, 2007, **46**, 7044; (b) A. Kumara, S.-S. Suna and A. J. Lees, *Coord. Chem. Rev.*, 2008, **252**, 922; (c) T. Ema, D. Tanida, K. Hamada and T. Sakai, *J. Org. Chem.*, 2008, **73**, 9129.
- For selected examples see: (a) A. Moretto, M. Crisma, F. Formaggio and T. Claudio, *Biopolymers*, 2010, **94**, 721; (b) M.-X. Wang, *Chem. Commun.*, 2008, 4541; (c) M. J. MacLachlan, *Pure Appl. Chem.*, 2006, **78**, 873.
- For selected examples see: (a) P. Ballester *et al.*, *J. Org. Chem.*, 2005, **70**, 6616; (b) C. A. Schalley, H. T. Baytekin and B. Baytekin, *Macrocyclic Chemistry*, 2005, 37; (c) K. Balakrishnan *et al.*, *J. Am. Chem. Soc.*, 2006, **128**, 6576.
- W. Brandt, V. J. Haupt and L. A. Wessjohann, *Curr. Top. Med. Chem.*, 2010, **10**, 1361.
- R. M. Wenger, *Progress in the Chemistry of Organic Natural Products*, 1986, **50**, 123.
- C. A. Lipinski, F. I. Lombardo, B. W. Dominy and P. J. Feeney, *Adv. Drug Delivery Rev.*, 1997, **23**, 3.
- (a) E. M. Driggers, S. P. Hale, J. Jinbo Lee and N. K. Terrett, *Nat. Rev. Drug Discovery*, 2007, **7**, 608; (b) E. Marsault and M. L. Peterson, *J. Med. Chem.*, 2011, **54**, 1961.
- J. A. Wells and L. McClendon, *Nature*, 2007, **450**, 1001.
- A. Macchioni, G. Ciancaleoni, C. Zuccaccia and D. Zuccaccia, *Chem. Soc. Rev.*, 2008, **37**, 479.
- (a) R. Ozisik, E. D. von Meerwall and W. L. Mattice, *Polymer*, 2002, **43**, 629; (b) C. J. C. Edwards, R. F. T. Stepto and J. A. Semlyen, *Polymer*, 1980, **21**, 781; (c) C. J. C. Edwards, R. F. T. Stepto and J. A. Semlyen, *Polymer*, 1982, **23**, 865; (d) M. Fukatsu and M. Kurata, *J. Chem. Phys.*, 1966, **44**, 4539.
- (a) F. W. Okumu, G. M. Pauletti, D. G. Vander Velde, T. J. Siahhan and R. T. Borchardt, *Pharm. Res.*, 1997, **14**, 169; (b) B. Wang *et al.*, *J. Pept. Res.*, 1999, **53**; (c) H. T. He, C. R. Xu, X. Song and T. J. Siahhan, *J. Pept. Res.*, 2003, **61**, 331.
- For recent examples of generating acyclic controls of macrocycles using this strategy see: (a) D. G. Udugamasooriya and M. R. Spaller, *Biopolymers*, 2008, **89**, 653; (b) J. E. DeLorbe, J. H. Clements, B. B. Whiddon and S. F. Martin, *ACS Med. Chem. Lett.*, 2010, **1**, 448.
- D. Wu, A. Chen and C. S. Johnson, *J. Magn. Reson., Ser. A*, 1995, **115**, 260.
- A. R. Bogdan and K. James, *Chem.–Eur. J.*, 2010, **16**, 14506.
- $\log D_{7.4}$  is defined as the logarithm of the partition coefficient between 1-octanol and an aqueous buffer at pH 7.4.
- P. D. Leeson and J. R. Empfield, *Annu. Rep. Med. Chem.*, 2010, **45**, 393.
- A. R. Bogdan and N. Sach, *Adv. Synth. Catal.*, 2009, **351**, 849.
- $D$  = diffusion coefficient,  $T$  = temperature,  $k$  = Boltzmann constant,  $\eta$  = solvent viscosity and  $r_H$  = hydrodynamic radius.
- J. Vinograd, J. Liebowitz, R. Radloff and P. Laipis, *Proc. Natl. Acad. Sci. U. S. A.*, 1965, **53**, 1104.
- A. D. Hershey, E. Burgi and L. Ingram, *Proc. Natl. Acad. Sci. U. S. A.*, 1963, **49**, 748.
- D. H. Rich, *Perspect. Med. Chem.*, 1993, 15.
- S. Augé *et al.*, *J. Phys. Chem. B*, 2009, **113**, 1914.
- See ref. 17 for details of the preparation of this compound.
- G. S. Kapur, E. J. Cabrita and S. Berger, *Tetrahedron Lett.*, 2000, **41**, 7181.
- Bruker, *DOSY and Diffusion by NMR, A Tutorial for Topspin 2.0, Version 2.0.0*, Rheinstetten, Germany, 2006.
- M. Findeisen, T. Brand and S. Berger, *Magn. Reson. Chem.*, 2007, **45**, 175.